
This is an electronic reprint of the original article.
This reprint may differ from the original in pagination and typographic detail.

Partl, Gabriel Julian; Naier, Benjamin Florian Erich; Bakry, Rania; Schlapp-Hackl, Inge; Kopacka, Holger; Wurst, Klaus; Gelbrich, Thomas; Fliri, Lukas; Schottenberger, Herwig
Can't touch this: Highly omniphobic coatings based on self-textured C6-fluoroponytailed polyvinylimidazolium monoliths

Published in:
Journal of Fluorine Chemistry

DOI:
[10.1016/j.jfluchem.2021.109839](https://doi.org/10.1016/j.jfluchem.2021.109839)

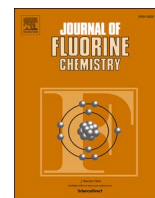
Published: 01/09/2021

Document Version
Publisher's PDF, also known as Version of record

Published under the following license:
CC BY

Please cite the original version:
Partl, G. J., Naier, B. F. E., Bakry, R., Schlapp-Hackl, I., Kopacka, H., Wurst, K., Gelbrich, T., Fliri, L., & Schottenberger, H. (2021). Can't touch this: Highly omniphobic coatings based on self-textured C6-fluoroponytailed polyvinylimidazolium monoliths. *Journal of Fluorine Chemistry*, 249, Article 109839. <https://doi.org/10.1016/j.jfluchem.2021.109839>

This material is protected by copyright and other intellectual property rights, and duplication or sale of all or part of any of the repository collections is not permitted, except that material may be duplicated by you for your research use or educational purposes in electronic or print form. You must obtain permission for any other use. Electronic or print copies may not be offered, whether for sale or otherwise to anyone who is not an authorised user.



Can't touch this: Highly omniphobic coatings based on self-textured C6-fluoroponytailed polyvinylimidazolium monoliths

Gabriel Julian Partl^{a,1}, Benjamin Florian Erich Naier^{a,1}, Rania Bakry^{b,1}, Inge Schlapp-Hackl^{a,c}, Holger Kopacka^a, Klaus Wurst^a, Thomas Gelbrich^d, Lukas Fliri^{a,c,*}, Herwig Schottenberger^{a,*}

^a Institute of General, Inorganic and Theoretical Chemistry, Leopold-Franzens-University Innsbruck, Innrain 80-82, A-6020 Innsbruck, Austria

^b Institute of Analytical Chemistry, Leopold-Franzens-University Innsbruck, Innrain 80-82, A-6020 Innsbruck, Austria

^c Department of Bioproducts and Biosystems, Aalto University, P.O. Box 16300, 00076 Aalto, Finland

^d Institute of Pharmacy, Pharmaceutical Technology, Leopold-Franzens-University Innsbruck, Innrain 52c, A-6020 Innsbruck, Austria

ARTICLE INFO

Keywords:
Omniphobic
Coatings
Self-assembly
Fluoroponytails
Polyvinylimidazolium

ABSTRACT

The quaternization of 1-vinylimidazole with 1*H*,1*H*,2*H*,2*H*-perfluorooctyl iodide, followed by anion metathesis reactions, allowed for the synthetic access of novel polymerizable fluorosurfactant salts with excellent yields, scalable from multigram up to bulk quantities on the kg scale. Subsequently, a series of doubly fluoroponytailed monomers as well as bridged bis-vinylimidazolium cross-linkers have been prepared via expedient thionation / *S*-alkylation. Thus, the resulting pool of these late stage intermediates offers great potential in task-specific surface tuning. Through polymerization in appropriate porogen mixtures combined with the micellar self-aggregation of the perfluoroalkyl moieties along with synergistic ionic interactions of the novel fluorosurfactants, the formation of nano-scalar monolithic structures is induced as evidenced by SEM imaging. According to contact angle measurements, the lotus-like textures hereby created drastically enhance oil and water repellency of the resulting polymer surface. Heeding the well-established cooperative concepts of chemical surface functionalization, accompanied by physical roughness, represents a proven strategy to impart high omniphobicity. However, the applicative maturity of systems based on nanophysics is frequently restricted by tedious and intricate patterning techniques as well as the environmental constraints of surface-active fluoroorganic compounds, on which high-performance systems indispensably rely.

1. Introduction

Due to a variety of unique properties, including excellent water and oil repellency [1], high thermal stability, remarkable oxygen affinity, as well as excellent surfactant properties [2–4], the substance class of perfluorinated and polyfluorinated compounds (PFCs) is found in a broad portfolio of both industrial and consumer-use products [5–12]. Most of the desired features of the compounds are attributed to affinity-driven self-orientation of their perfluoroalkyl residues owing to F–F interactions. The extent of such effects was found to be strongly dependent on the number of repetitive CF₂-segments, with a critical number of eight perfluorinated carbons as lower limit to obtain sufficient “side-chain crystallinity” of the supramolecular structures [13]. Unfortunately, these same properties, in combination with the compounds' general persistency, lead to bioaccumulation in the

environment. For example, it was shown that almost all human blood samples collected worldwide by the early 2000s contained measurable quantities of various long chain PFCs [14–16]. Due to their (eco) toxicity [17] and their probable linkage to various diseases [18], many of the C8 PFCs have consequently been classified as “substances of very high concern” (SVHCs) and / or “very persistent, very bioaccumulative” (vPvB) chemicals and are currently being phased out from commercial applications [19].

Nonetheless, the outstanding properties of perfluoroalkylated compounds cannot yet be adequately achieved by common chemicals [20], e.g. in applications for sterile medical clothing [21], giving rise to the search for more eco-friendly alternatives. In the case of fluorocarbon chemistry – although admittedly disputed [22] – these can be found in derivatives bearing a perfluorohexylethyl (C₂H₄–C₆F₁₃) side chain, as both bioaccumulation as well as systemic toxicity tend to decrease with

* Corresponding authors.

E-mail addresses: lukas.fliri@aalto.fi (L. Fliri), herwig.schottenberger@uibk.ac.at (H. Schottenberger).

¹ Connoted authors have contributed equally to this work.

shortening PFC chain length and the introduction of a C₂H₄ hydrocarbon spacer [20,23]. A hereby implicated loss in self-ordering by virtue of attenuated F – F contacts can be compensated by exploiting supramolecular phenomena of self-organization through molecular tailoring in the fluorine-free backbone (see Fig. 1). The feasibility of this approach was recently demonstrated by our group, showcasing π – π contacts in self-aggregating fluoroonytailed dyes [24–26] or ionic interactions in imidazolium-based fluorosurfactants [27]. Starting from the highly affordable industrial educt 1-vinylimidazole, ionic fluoroonytailed monomers – closely related to previously published derivatives [27] – were synthesized in order to evaluate the influence of the above-mentioned supramolecular aggregation displayed by environmentally preferable polymers based on 1-vinylimidazolium salts [28–31].

In general, fluorine containing polymers – with the exception of PTFE, ETFE and PVDF – are restricted to high performance or niche applications [32,33] and mostly consist of copolymers based on neutral perfluorinated (meth)acrylates [32,34,35] which inherently exhibit handling drawbacks caused by their toxicity, very high reactivity and relatively complex monomer preparation chemistry [35]. In this contribution, the potential of imidazolium-based fluoroonytailed polymers is demonstrated by preparing omniphobic coatings – repelling both oil and water – for silica and, in particular, glass substrates. According to conceptions of the renowned “lotus effect” [36], it is common knowledge that surface wettability is drastically affected by its micro- or nanostructures [37–39], thus stimulating a huge variety of approaches for their artificial generation [40–48]. This, however, generally depends on complex and time-consuming procedures [39,49,50]. A straightforward method to create nano-scaled monolithic structures [51–53] was achieved by the inclusion of porogens into the polymerization mixtures. However, this is restricted to monomers with suitable solubility profiles. As these can be readily adjusted for cationic monomers via anion metathesis, this strategy, especially in combination with the tendency of self-orientation of the polyfluorinated moieties, became feasible. Interestingly, by starting from the same pool of monomer intermediates, this synergistic interplay facilitates not only the implementation of omniphobicity, but also hydrophilic oleophobicity [54], which, for example, is of high relevance for oil-water separation or the adsorptive removal of PFC-pollutants such as perfluorooctanoic acid (PFOA) or perfluorooctanesulfonic acid (PFOS) from aquatic environments. Furthermore, numerous other possible applications such as fouling suppression or anti-icing measures are claimed and discussed in detail in the respective recent patent literature [55–58].

2. Results and discussion

2.1. Monomer synthesis and properties

The synthetic procedures for the preparation of the imidazolium-based fluoroonytailed monomers (**1a** – **3b**) as well as the novel cross-linkers (**4** – **6b**) are summarized in Scheme 1. Imidazoline-2-thiones **2** and **5** were prepared based on classic procedures [59,60]. Cross-linker precursor **4** was synthesized in accordance with literature [61] with some adjustments for large scale preparations. Although seemingly representing a straightforward quaternization reaction, the *N*-alkylation of 1-vinylimidazole proved to be problematic in practice due to self-polymerization tendencies of the vinyl-group leading to shortcomings in product yield and purity. We found that this side reaction can be elegantly suppressed by applying neat reaction conditions and purposefully performing the reaction in ambient atmosphere, allowing for the isolation of **1a** in 76% yield. It is believed that this outcome is due to the high O₂ affinity of the PFC-moieties, which caused the partial oxidative formation of iodine radicals, thus additionally interfering with free-radical polymerization reactions [62,63]. Neat conditions were also preferable for the preparation of **3a** (93% yield, compared to < 50% when using MeCN as solvent), but could not be applied in the synthesis of cross-linker **6a** due to solubility issues.

Imidazolium iodides (**1a**, **3a** and **6a**) were further transformed to their chloride analogues (**1b**, **3b** and **6b**). Although comparatively expensive, a simple metathesis protocol applying solid AgCl in MeOH was utilized, allowing for almost quantitative yields. Pretrials with freshly prepared CuCl gave similar results, however rigorous exclusion of water and oxygen were necessary to avoid product discoloration due to cupric contamination.

As evidenced by the comparison of **1a** and **1b** in Table 1, the choice of anions in the presented systems drastically alters their solubility profile. By exchanging iodide for chloride, the solubility in aqueous environments was increased 90-fold, thus giving preferential properties for the porogen-assisted preparation of the coating mixtures (see Table 2). Moreover, possible polymerization interferences from the iodide ion [62,63] are thereby minimized. The exchange of anion also resulted in measurable solubilities in H₂O for relatively fluorine-rich doubly fluoroonytailed monomer **3b** as well as cross-linker **6b**, thus making them accessible for water-based polymerization protocols. However, short chain alcohols are better suited solvents for these compounds.

Furthermore, the concentration-dependent aqueous surface tension of chloride containing monomers **1b**, **3b** and **6b** was measured (see ESI

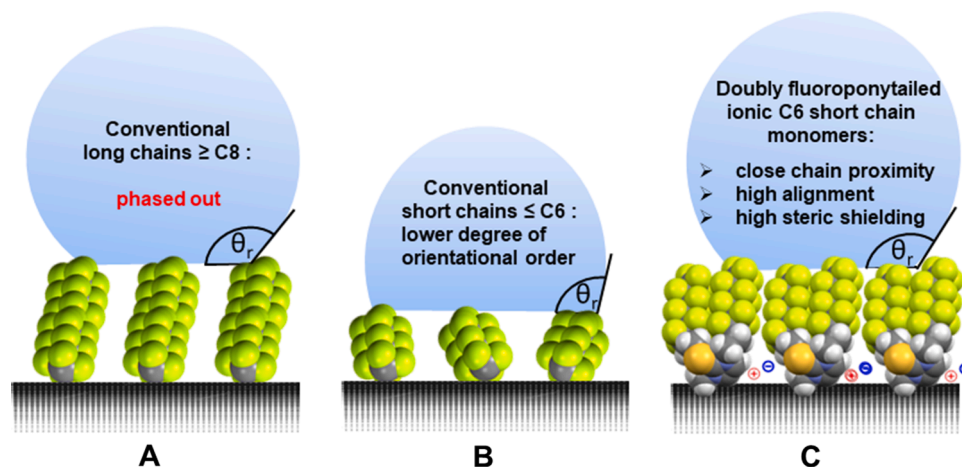
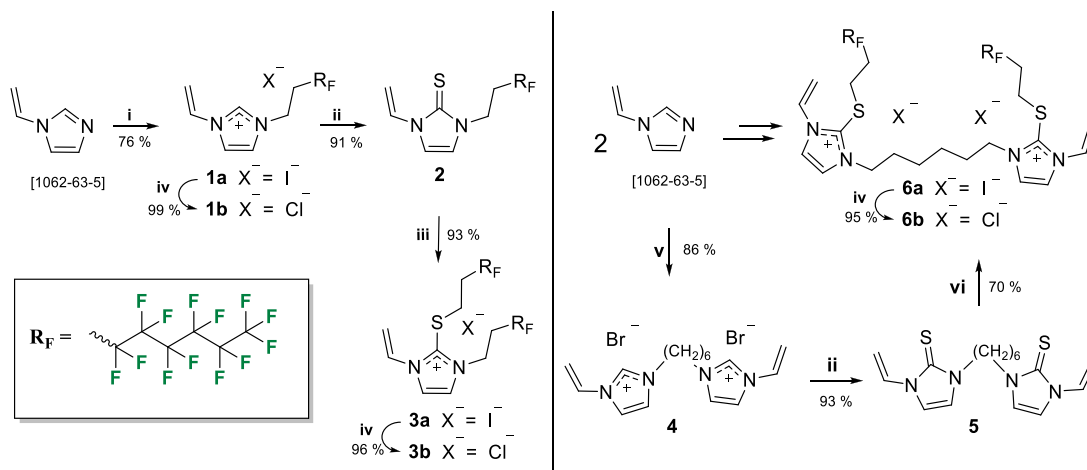


Fig. 1. Comparison between wettability properties of A: phased out systems containing long chain perfluorocarbons; B: less hazardous but also less oriented short chain perfluorocarbons; C: our proposed concept of short chain monomers stabilized by ionic interactions, resulting in environmentally more acceptable high-performance surface modifications.



Conditions: i) $R_F(CH_2)_2I$, neat 72 h, 70 °C; ii) K_2CO_3 / S_8 , MeOH 3h, reflux; iii) $R_F(CH_2)_2I$, neat 20 h, 110 °C; iv) $AgCl$, MeOH, RT; v) $Br(CH_2)_6Br$, neat 36 h, 0 to 5 °C; vi) $R_F(CH_2)_2I$, MeCN 48 h, reflux

Scheme 1. Summary and conditions of the applied synthetic procedures.

Table 1

Apparent solubilities of the synthesized monomers **1a**, **1b** and **3b** as well as cross-linkers **2** and **6b** in selected solvents in $g L^{-1}$.

	1a	1b	2	3b	6b
H ₂ O	10	900	–	~8	20
MeOH	360	>1000	180	>1000	>1000
EtOH	650	>1000	100	250	>1000
DMF	>1000	30	> 1000	30	>1000
THF	–	–	> 1000	~2.5	–
Et ₂ O	–	–	200	–	–
Toluene	–	–	150	–	–
n-Heptane	–	–	–	–	–

Figure S1 and Table S1). Compared to similar compounds [27], surface tension values of **1b** are markedly higher than expected, especially in relation to N–H protic congeners. The dimer salt **6b**, too, shows relatively high values in comparison to literature [64]. As expected, monomer **3b**, bearing two fluorinated chains, reduces the surface tension of water most effectively and efficiently (15.04 mN/m at the critical micelle concentration of 0.29 mmol/l or 0.025 wt%), thus outclassing common fluorosurfactants such as PFOA or PFOS.

2.2. Solid-state structures

Despite the generally reluctant crystallization behavior of fluoro-ponytail compounds, it was possible to confirm the chemical compositions of two monomers by single crystal structure determination. Suitable single crystals of chloride **1b** were cropped upon slow vapor diffusion of diethyl ether into its ethanolic solution at 4 °C. In contrast, a solid form containing the iodide **1a** was obtained after the addition of equimolar amounts of perfluoroethyl iodide to an ethanolic solution, resulting in the formation of the σ -hole complex **1a**• $C_8F_{17}I$. The asymmetric unit of **1b** contains two formula units (Fig. 2, top left). The conformation of the alkyl chain of the cation can be characterized in terms of a sequence of six torsion angles, i.e. N–C–C–C (henceforth denoted as t_1) and C–C–C–C (t_2 to t_6). In the first cation unit of **1b**, t_1 is *gauche* and the rest of the chain is all-*trans*. This chain geometry differs from that in the other cation unit where t_3 is *gauche* and all other torsions are *trans*. Additionally, this latter chain is disordered over two orientations which belong to the same principle conformation. Within the crystal structure, the fluoroalkyl chains of neighboring cations are stacked in a parallel fashion. This in turn results in a sequence of alternating perfluoroalkyl ponytail and polar domains parallel to the *ab*

plane (Fig. 2, bottom left).

The asymmetric unit of **1a**• $C_8F_{17}I$ contains two formula units. Both independent $C_8F_{17}I$ molecules display an all-*trans* conformation, and the alkyl chain of one independent cation is also all-*trans* (Fig. 2, top right). A slightly different geometry is found in the second cation unit, with t_1 (N–C–C–C) being *gauche* and all of t_2 to t_6 being *trans*. Three of the four independent perfluoroalkyl chains present in this structure were found to be disordered between two slightly different orientations. As observed for **1b**, neighbouring fluoroalkyl chains in the crystal structure of **1a**• $C_8F_{17}I$ are aligned in a parallel fashion. This particular supramolecular arrangement results in alternating perfluoroalkyl ponytail and polar domains which extend parallel to the *ab* plane (Fig. 2, bottom right). The σ -hole complex displays halogen bonding between the iodide counter ion and the 1-iodoperfluoroalkane guest with $I \cdots I$ separations of 3.366(1) and 3.460(1) Å and exemplifies the strong tendency of PFCs for self-assembly [65], here involving perfluoroalkyl units of opposite charge

An investigation of a crystal of **3a** indicated a monoclinic structure with the space group symmetry $P2_1/c$. The obtained structure solution is consistent with the expected connectivity of the compound and shows an asymmetric unit containing seven formula units. Unfortunately, the quality of the data was not sufficient to establish a reliable model for the 14 independent and severely disordered $-C_6F_{13}$ chain fragments in this structure.

2.3. Polymer coatings – SEM imaging and contact angle measurements

To investigate the influences of the synthesized compounds on structure and wettability of silica surface modifications, coatings I–IV were prepared. The polymerization was carried out through an in-situ free radical photoinitiated polymerization. The respective composition specifics are listed in Table 2. For coatings I, III and IV, the cross-linker ethylene glycol dimethacrylate (EGDMA) [52] was chosen to examine the effects of counter ions as well as fluorine content introduced by the different monomers **1a**, **1b** and **3b** (see Table 2). In order to gauge the influence of the cross-linker on overall performance, for II, fluoro-ponytail cross-linker **6b** was reacted with **1a**. To achieve rigid porous structures, the polymerization mixtures were selected depending on the solubilities of the monomers, cross-linkers and the polymer-particles formed through radical polymerization in the early phase of the process. Of course, the presented systems allow for a much broader scope of combinations, however optimization of the properties would have exceeded the scope of this study.

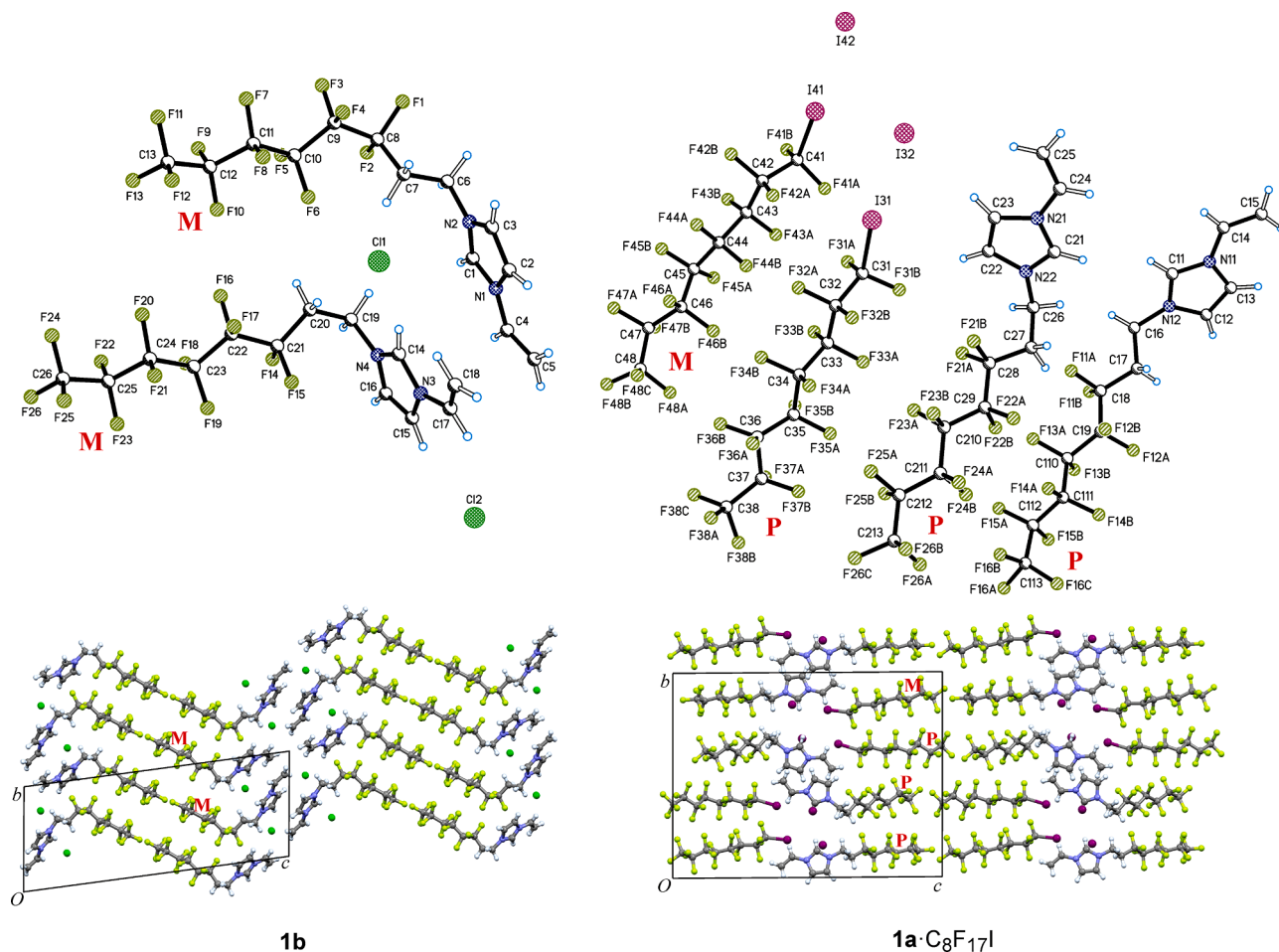


Fig. 2. Top: Asymmetric units of **1b** (left) and **1a**·C₈F₁₇I (right). The bottom row shows the corresponding crystal packing arrangements, with each structure being viewed along the crystallographic *a* axis. Minor disorder components are omitted for clarity. The helicity (M- or P-configuration) of perfluoroalkyl chains is denoted by the letters M and P. In **1b**, all contacts between perfluoroalkyl chains along their longitudinal axes involve chains of the same helicity (i.e. MM or PP in *ab* planes). By contrast, the corresponding contact sequences along the *b* axis of **1a**·C₈F₁₇I are PPPM and MMMP.

Table 2

Composition specifics for coatings I-IV.

Entry	Monomer	Cross-linker	Solvent mixture
I	100 mg 3b	100 μl EGDMA	125 μl 1-PrOH/ 125 μl MeCN/ 50 μl H ₂ O
II	100 mg 1a	100 mg 6b	125 μl 1-PrOH/ 125 μl MeCN/ 50 μl H ₂ O
III	85 mg 1a	100 μl EGDMA	125 μl 1-PrOH/ 125 μl MeCN/ 65 μl H ₂ O
IV	100 mg 1b	100 μl EGDMA	125 μl 1-PrOH/ 125 μl MeCN/ 50 μl H ₂ O

Radical starter: 10 mg 2,2-dimethoxy-2-phenylacetophenone, EGDMA = ethylene glycol dimethacrylate.

SEM images of I-IV (see Fig. 3) show that the primary polymerization particles form aggregates of varying height, creating a very fine, arguably pseudo-hierarchical architecture and resulting in the desired nanostructure that naturally repels liquids [66]. It is well known that in order to generate a super-omniphobic surface, its physical structure is absolutely critical. In fact, through intricate structural engineering, highly omniphobic surfaces may be created without relying on any fluorocarbon chemistry at all [67,68].

In terms of the morphological structure of the monolithic layer, all coatings exhibit a typical porous scaffold with small globule sizes and interconnected coalescence of globules to form polymer clusters. Comparison of mixtures I – with **3b** as monomer – and polymer IV generated from **1b**, shows that the attachment of two fluoronyltails to the vinylimidazolium core results in a denser structure, which can be correlated to the higher fluorine content. II with **6b** as cross-linker

results in a non-uniform structure, presumably because of steric demand introduced by the bulky shape of **6b**. The presence of iodide in III enlarged the cavities between the globules, which can be attributed to both, its negative effect on the polymerization kinetics and phase inversion [62,63], as well as to its binding to micellar interfaces reported for similar non-fluorinated imidazolium compounds [69].

The consequences of the different morphologies become noticeable in the measured contact angles for coatings I-IV, which are listed in Table 3. All surfaces are superhydrophobic (contact angle > 150°), which is likely attributable to the liquid-repellant nanostructure of the polymers as well as to a high degree of side-chain crystallization and fluorine chain organization. The extreme hydrophobicity is still somewhat unexpected insofar that polyionic species would normally be less hydrophobic or even, as reported for chloride containing imidazolium co-polymers [70], hydrophilic. Except for III, all surfaces display diiodomethane and n-hexadecane angles >150°

Especially coatings I and II display extremely high contact angles for CH₂I₂ droplets. Expectedly, the richer the monoliths are in perfluorinated moieties, the more omniphobic they tend to be: II, having the highest content of perfluorinated groups, arguably features the best repellent properties, while III exhibits comparatively poorer ones. In fact, during determination of the CH₂I₂ contact angle on coating II, the droplet had to be pressed onto the surface numerous times because it tenaciously refused to adhere to it (see Fig. 4 and the video file in the ESI). Comparing I and IV, a similar effect is observable: while both contain the same amount of a chloride salt monomer, the monomer in I

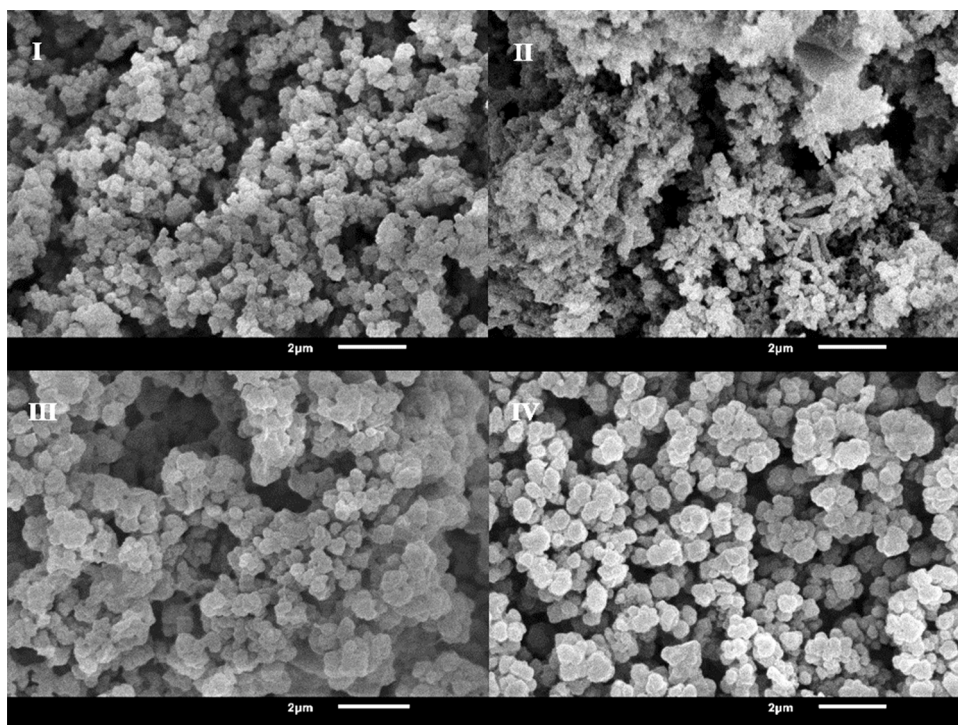


Fig. 3. SEM images of coatings I-IV. Primary particles in I and IV are spherical in nature; in II, they are rod-like and in III, they are platelet-shaped.

Table 3

Contact angles for omniphobic coatings I-IV. Numbers in brackets show the respective standard deviations.

Entry	Contact angle water/air [°]	Contact angle CH ₂ I ₂ /air [°]	Contact angle C ₁₆ H ₃₄ /air [°]
I	168.96 (1.80)	170.36 (0.68)	151.85 (2.68)
II	168.96 (1.69)	171.83 (0.35)	150.71 (0.48)
III	162.14 (0.39)	147.46 (1.62)	142.98 (0.94)
IV	165.27 (0.71)	165.60 (0.45)	150.59 (0.54)

(3b) is doubly fluorinated and observably better suited for creating omniphobic properties. In reference to IV, the water/air contact angle is approximately 4° higher, and for CH₂I₂/air contact angles, a 5° increase is achieved.

In literature, branched C6-C7 fluoroacrylate homopolymer coatings with water contact angles of 107–117° and n-hexadecane contact angles of 68–74° [71] are featured. Coatings made from polymers with fluorinated backbones, such as Teflon® AF, are more hydrophobic with 125° (advancing angle) for water and 69° (advancing angle) for n-hexadecane. Pure fluorodecyl polyhedral oligomeric silsesquioxane (F-POSS) films exhibit good hydro- and oleophobicity with 124°

(advancing angle, water) and 80° (advancing angle, n-hexadecane) as well [72].

Taking into account that the fluorine content in surface modifications I-IV is lower than in the examples discussed above, it is apparent that their extreme omniphobicity is not achieved purely through chemical composition, rather polymer architecture as well. Interestingly, coatings I-IV exhibit wetting behavior strikingly similar to post-fluorinated hierarchically structured surfaces such as porous silicon films [73], grafted silica microparticles [74], alumina nanowire forests [75] or titanium dioxide nanotubes on titanium micropillars [76], while being significantly simpler to manufacture.

3. Conclusions and outlook

In line with growing global scrutiny towards bioaccumulative long chain PFCs, we were intrigued to design a new generation of environmentally more acceptable, non-volatile C6-fluorosurfactants. Such paradigmatic assortments of monomers, cross-linkers and polymers around 1-vinylimidazole and related heterocycles represent a versatile systematic starting base, even though less than six carbon atoms per unit still need to retain some of the unique features of longer perfluoroalkyl chains [77]. Notably, in the realm of imidazoles, exhaustive substitution

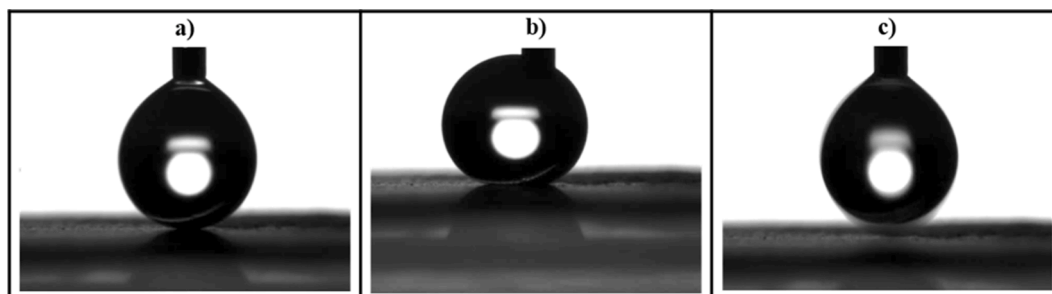


Fig. 4. a) CH₂I₂ droplet, suspended from a needle, moving towards surface coating II. b) droplet is pressed down onto the surface. c) instead of adhering to the surface, the droplet sticks to the needle and moves upwards with it again.

chemistry is straightforward and equals less affordable concepts of ecological compatibilisation such as fluorous short-chain branching [78] since the small organic core can be considered a crowded nodal point on its own. Moreover, it is foreseeable that the applicative indispensability of the fluorous effect in various high-end fields will give rise to significantly more exceptional scientific outcome [79].

4. Experimental

4.1. Monomer synthesis and solubility data

Reagents and solvents were purchased from Sigma-Aldrich, Merck or Fluka in the highest purity available and used as received unless stated otherwise. 1*H*,1*H*,2*H*,2*H*-Perfluorooctyl iodide, when applied in excess, can be recycled via distillation and reused. ¹³C and ¹H NMR spectra were recorded with a Bruker Avance DPX 300 spectrometer. FT-IR spectra were measured with a Bruker ALPHA-P FT spectrometer in ATR mode. Cross-linker intermediate **4** was prepared according to literature [61] with slight modifications; the modified procedure was already described in a similar project [51]. Structures of imidazoline thiones **2** and **5** were determined using single crystal X-ray diffractometry and were recently discussed in detail in independent data communications [80,81]. For convenience, procedures and characterizations for all required compounds are summarized in the Supporting Information.

A simple, approximative solubility-study was conducted for monomers **1a**, **1b** and **3b** as well as for intermediate **2** and cross-linker **6b** (see Table 1). Specifically, the compounds were added to 10 mL of solvent in 10 mg increments at room temperature (25 °C) and stirred until the liquid phase was saturated and a solid residue was visible.

4.2. Single crystal structure determination

Diffraction intensity data were recorded with a Bruker D8 Quest Photon 100 diffractometer using MoK α ($\lambda = 0.71073$ Å) radiation. The crystal structures were solved by direct methods and refined by full-matrix least-squares techniques [82,83].

1a•C₈F₁₇I [(C₁₃H₁₀F₁₃N₂)⁺T⁻ • C₈F₁₇I]: empirical formula C₂₁H₁₀F₃₀I₂N₂; formula weight 1114.11; $T = 210(2)$ K; triclinic space group $P\bar{1}$; $Z = 4$; unit cell parameters $a = 7.0304(3)$ Å, $b = 19.2345(8)$ Å, $c = 25.3712(12)$ Å, $\alpha = 89.5480(10)^\circ$, $\beta = 85.7730(10)^\circ$, $\gamma = 87.9540(10)^\circ$, $V = 3419.3(3)$ Å³; 55,435 reflections collected; 12,433 independent reflections ($R_{\text{int}} = 0.0331$); $R1 [I > 2\sigma(I)] = 0.0689$; $wR2$ (all data) = 0.2066.

1b [(C₁₃H₁₀F₁₃N₂)⁺Cl⁻]: empirical formula C₁₃H₁₀ClF₁₃N₂; formula weight 476.68; $T = 173(2)$ K; triclinic space group $P\bar{1}$; $Z = 4$; unit cell parameters $a = 6.1826(7)$ Å, $b = 10.6109(13)$ Å, $c = 26.966(3)$ Å, $\alpha = 82.021(3)^\circ$, $\beta = 87.902(3)^\circ$, $\gamma = 86.111(3)^\circ$, $V = 1747.2(4)$ Å³; 29,913 reflections collected; 6406 independent reflections ($R_{\text{int}} = 0.0404$); $R1 [I > 2\sigma(I)] = 0.0633$; $wR2$ (all data) = 0.1691.

CCDC 2079139-40 contain the supplementary crystallographic data for this paper. These data can be obtained free of charge from the Cambridge Crystallographic Data centre via www.ccdc.cam.ac.uk/data_request/cif.

3a [(C₂₁H₁₃F₂₆N₂S)⁺T⁻] (unit cell data only): $T = 183(2)$ K; monoclinic space group $P2_1/c$; $Z = 28$ and $Z' = 7$; unit cell parameters $a = 31.428(3)$ Å, $b = 12.0843(10)$ Å, $c = 60.106(5)$ Å, $\alpha = \gamma = 90^\circ$, $\beta = 99.596(3)^\circ$, $V = 22,508(3)$ Å³.

4.3. Surface tension measurements

The surface tension of aqueous solutions of selected monomers was recorded using the drop shape analysis instrument Krüss DSA25E, equipped with illumination, a height adjustable desk, video camera and Advance 1.4.2 software (Krüss, D-Hamburg, Germany). Using the pendant drop technique at ambient conditions (24–25 °C, 20 RH%), the

surface tension of all aqueous solutions was measured in series of 10 drops each. The drop was suspended from a needle (outside diameter: 1.83 mm) and the drop volume increased by a dosimeter. A recommended B-value (0.4 to 0.6), computed constantly by the software, allowed for a proper adjustment of the drop volume.

4.4. Sample pretreatment and polymer synthesis

Glass priming and monolithic layer preparation were carried out according to published procedures [52,53].

Glass priming: The glass plates were rinsed with acetone and H₂O, activated with aqueous NaOH (0.2 M; 30 min), washed with H₂O followed by immersion in hydrochloric acid (0.2 M; 30 min), then again washed with H₂O and finally washed with acetone. Thereafter, the plates were dried at 60 °C for 1 h. Glass surface activation was achieved by immersion in a solution of 3-(trimethoxysilyl)propyl methacrylate (20 vol.%) in 95% EtOH (pH adjusted to 5 with HOAc) for 2 h. The modified plates were washed with EtOH and dried for 24 h at RT.

Preparation of the monolithic layer: A Teflon gasket with a desired thickness ranging from 50 to 150 μm was placed on top of the modified glass plate, covered with another glass plate and clamped. The different polymerization mixtures were prepared according to Table 2 and ultrasonicated by means of an ultrasonic bath (5 min), before they were transferred into the assembled mold using a syringe and exposed to UV light for 30 min using a 254 nm lamp (8 \times 8 W lamps; UVP CX 2000 UV Crosslinker, Cambridge, UK). After the polymerization process was complete, the mold was disassembled. The monoliths attached to the plate surface were washed with MeOH and placed in a beaker filled with MeOH for 2 h, then air-dried to give samples I-IV.

4.5. Contact angle measurements

The contact angles of the coatings were recorded using the drop shape analysis instrument Krüss DSA25E in combination with a height-adjustable desk, video camera and Advance 1.4.2 software (Krüss, D-Hamburg, Germany). All experiments were performed under ambient conditions (24–25 °C, 20% room humidity). The contact angles of all coatings were measured in series of 3 drops each. The drop was suspended from a needle, using different volumes of water, hexadecane and diiodomethane. As fit method, the Young Laplace method was used. Obtained results and standard deviations are listed in Table 3.

4.6. SEM imaging

SEM pictures were taken with a JEOL JSM-6010 LV scanning electron microscope equipped with an energy dispersive detector (BRUKER, software: Esprit 1.9). All samples were sputtered with gold before being viewed under the microscope.

CRedit authorship contribution statement

Gabriel Julian Partl: Conceptualization, Data curation, Formal analysis, Validation, Writing – original draft, Writing – review & editing. **Benjamin Florian Erich Naier:** Conceptualization, Data curation, Formal analysis, Writing – original draft. **Rania Bakry:** Conceptualization, Data curation, Formal analysis. **Inge Schlapp-Hackl:** Data curation, Formal analysis. **Holger Kopacka:** Data curation, Formal analysis. **Klaus Wurst:** Data curation, Formal analysis. **Thomas Gelbrich:** Formal analysis, Writing – original draft, Visualization. **Lukas Fliri:** Writing – original draft, Conceptualization, Visualization, Writing – review & editing. **Herwig Schottenberger:** Conceptualization, Validation, Visualization, Writing – review & editing, Supervision.

Declaration of Competing Interest

There are no conflicts to declare.

Acknowledgements

We are grateful for financial support by the Austrian promotional bank under project 1621682 (Sustainable Textile Finishing -Water and Dirt Repellent Textile Impregnation).

Supplementary materials

Supplementary material associated with this article can be found, in the online version, at doi:[10.1016/j.jfluchem.2021.109839](https://doi.org/10.1016/j.jfluchem.2021.109839).

References

- [1] D.R. Husted, A. H. Ahlbrecht, inventor; Minnesota Mining and Manufacturing Co, US. *N,N*-Bis(1,1 dihydroperfluoroalkyl) acylamides and Polymers thereof. Publication Date 1957/02/19. US. Patent US2782184A.
- [2] J.L.H. Johnson, M.C. Dolezal, A. Kerschen, T.O. Matsunaga, E.C. Unger, In vitro comparison of dodecafluoropentane (DDFP), perfluorodecalin (PFD), and perfluorocylbromide (PFOB) in the facilitation of oxygen exchange, *Artif. Cell. Blood Sub.* 37 (2009) 156–162, <https://doi.org/10.1080/10731190903043192>.
- [3] M.P. Krafft, J.G. Riess, Selected physicochemical aspects of poly- and perfluoroalkylated substances relevant to performance, environment and sustainability-part one, *Chemosphere* 129 (2015) 4–19, <https://doi.org/10.1016/j.chemosphere.2014.08.039>.
- [4] L.C. Clark, F. Gollan, Survival of mammals breathing organic liquids equilibrated with oxygen at atmospheric pressure, *Science* 152 (1966) 1755–1756, <https://doi.org/10.1126/science.152.3730.1755>.
- [5] A. Czajka, G. Hazell, J. Eastoe, Surfactants at the Design Limit, *Langmuir* 31 (2015) 8205–8217, <https://doi.org/10.1021/acs.langmuir.5b00336>.
- [6] A. Hagenars, I.J. Meyer, D. Herzke, B.G. Pardo, P. Martinez, M. Pabon, W. de Coen, D. Knape, The search for alternative aqueous film forming foams (AFFF) with a low environmental impact: physiological and transcriptomic effects of two Forafac® fluorosurfactants in turbot, *Aquat. Toxicol.* 104 (2011) 168–176, <https://doi.org/10.1016/j.aquatox.2011.04.012>.
- [7] P. Khanjani, A.W.T. King, G.J. Partl, L.-S. Johansson, M.A. Kostianen, R.H.A. Ras, Superhydrophobic Paper from Nanostructured Fluorinated Cellulose Esters, *ACS Appl. Mat. Inter.* 10 (2018) 11280–11288, <https://doi.org/10.1021/acsami.7b19310>.
- [8] P. Kirsch, *Modern Fluoroorganic Chemistry: Synthesis, Reactivity, Applications*, Wiley-VCH, Weinheim, 2013.
- [9] A. Milonitis, I.S. Bayer, E. Loth, Recent advances in oil-repellent surfaces, *Int. Mater. Rev.* 61 (2016) 101–126, <https://doi.org/10.1080/09506608.2015.1116492>.
- [10] U. Sayed, P. Dabhi, *Finishing of textiles with fluorocarbons. Waterproof and Water Repellent Textiles and Clothing*, Elsevier, 2014, pp. 139–152.
- [11] J. Song, O.J. Rojas, *PAPER CHEMISTRY: approaching super-hydrophobicity from cellulosic materials: a Review*, *Nord. Pulp Pap. Res. J.* 28 (2013) 216–238, <https://doi.org/10.3183/npprj-2013-28-02-p216-238>.
- [12] S. Subhash Lathe, A. Basavraj Gurav, C. Shridhar Maruti, R. Shrikant Vhatkar, Recent Progress in Preparation of Superhydrophobic Surfaces: a Review, *JSEMAT* 02 (2012) 76–94, <https://doi.org/10.4236/jsemat.2012.22014>.
- [13] K. Honda, M. Morita, H. Otsuka, A. Takahara, Molecular aggregation structure and surface properties of poly(fluoroalkyl acrylate) thin films, *Macromolecules* 38 (2005) 5699–5705, <https://doi.org/10.1021/ma050394k>.
- [14] G.W. Olsen, M.E. Ellefson, D.C. Mair, T.R. Church, C.L. Goldberg, R.M. Herron, Z. Medhdizadehkhaki, J.B. Nobiletti, J.A. Rios, W.K. Reagen, L.R. Zobel, Analysis of a homologous series of perfluorocarboxylates from American Red Cross adult blood donors, 2000–2001 and 2006, *Environ. Sci. Technol.* 45 (2011) 8022–8029, <https://doi.org/10.1021/es1043535>.
- [15] K. Kannan, S. Corsolini, J. Palandysz, G. Fillmann, K.S. Kumar, B.G. Loganathan, M. A. Mohd, J. Olivero, N. van Wouwe, J.H. Yang, K.M. Aldoust, Perfluorooctanesulfonate and related fluorochemicals in human blood from several countries, *Environ. Sci. Technol.* 38 (2004) 4489–4495, <https://doi.org/10.1021/es0493446>.
- [16] A.B. Lindstrom, M.J. Strynar, E.L. Libelo, Polyfluorinated compounds: past, present, and future, *Environ. Sci. Technol.* 45 (2011) 7954–7961, <https://doi.org/10.1021/es2011622>.
- [17] M.B. Murphy, E.I.H. Loi, K.Y. Kwok, P.K.S. Lam, Ecotoxicology of organofluorous compounds, in: I.T. Horváth (Ed.), *Top Curr Chem*, Springer-Verlag, Berlin Heidelberg, 2012, pp. 339–364, https://doi.org/10.1007/128_2011_273, 308.
- [18] S.J. Frisbee, A.P. Brooks, A. Maher, P. Flensburg, S. Arnold, T. Fletcher, K. Steenland, A. Shankar, S.S. Knox, C. Pollard, J.A. Halverson, V.M. Vieira, C. Jin, K.M. Leyden, A.M. Ducatman, The C8 health project: design, methods, and participants, *Environ. Health Persp.* 117 (2009) 1873–1882, <https://doi.org/10.1289/ehp.0800379>.
- [19] M. Land, C.A. de Wit, A. Bignert, I.T. Cousins, D. Herzke, J.H. Johansson, J. W. Martin, What is the effect of phasing out long-chain per- and polyfluoroalkyl substances on the concentrations of perfluoroalkyl acids and their precursors in the environment? A systematic review, *Environ. Evid.* 7 (2018), <https://doi.org/10.1186/s13750-017-0114-y>.
- [20] J.S. Bowman, Fluorotechnology is critical to modern life: the FluoroCouncil counterpoint to the Madrid Statement, *Environ. Health Persp.* 123 (2015) A112–A113, <https://doi.org/10.1289/ehp.1509910>.
- [21] S. Schellenberger, P.J. Hill, O. Levenstam, P. Gillgard, I.T. Cousins, M. Taylor, R. S. Blackburn, Highly fluorinated chemicals in functional textiles can be replaced by re-evaluating liquid repellency and end-user requirements, *J. Clean. Prod.* 217 (2019) 134–143, <https://doi.org/10.1016/j.jclepro.2019.01.160>.
- [22] S. Brendel, É. Fetter, C. Staudé, L. Vierke, A. Biegel-Engler, Short-chain perfluoroalkyl acids: environmental concerns and a regulatory strategy under REACH, *Environ. Sci. Eur.* 30 (2018) 9, <https://doi.org/10.1186/s12302-018-0134-4>.
- [23] R.C. Buck, J. Franklin, U. Berger, J.M. Conder, I.T. Cousins, P. de Voogt, A. A. Jensen, K. Kannan, S.A. Mabury, S.P.J. van Leeuwen, Perfluoroalkyl and polyfluoroalkyl substances in the environment: terminology, classification, and origins, *Integr. Environ. Assess.* 7 (2011) 513–541, <https://doi.org/10.1002/ieam.258>.
- [24] L. Fliri, G. Partl, D. Winkler, K. Wurst, T. Gelbrich, T. Müller, H. Schottenberger, M. Hummel, Ionic and neutral fluorosurfactants containing ferrocene moieties as chromophoric constituents, *J. Fluorine Chem.* 241 (2021), 109674, <https://doi.org/10.1016/j.jfluchem.2020.109674>.
- [25] L. Fliri, G. Partl, T. Gelbrich, V. Kahlenberg, G. Laus, H. Schottenberger, (E)-2,6-Dibromo-4-(2-(1-(1H,1H,2H,2H-perfluoroalkyl)pyridinium-4-ylethenyl)phenolate methanol disolvate, a fluoroonylated solvatochromic dye, *Acta Crystallogr. E* 73 (2017) 1526–1529, <https://doi.org/10.1107/S2056989017013378>.
- [26] L. Fliri, G. Partl, D. Winkler, G. Laus, T. Müller, H. Schottenberger, M. Hummel, Fluoroonylated Brooker's merocyanines: studies on solution behavior, solvatochromism and supramolecular aggregation, *Dyes Pigments* 184 (2021), 108798, <https://doi.org/10.1016/j.dyepig.2020.108798>.
- [27] M. Hummel, M. Markiewicz, S. Stolte, M. Noisternig, D.E. Braun, T. Gelbrich, U. J. Griesser, G. Partl, B. Naier, K. Wurst, B. Krüger, H. Kopacka, G. Laus, H. Huppertz, H. Schottenberger, Phase-out-compliant fluorosurfactants: unique methimidazolium derivatives including room temperature ionic liquids, *Green Chem* 19 (2017) 3225–3237, <https://doi.org/10.1039/C7GC00571G>.
- [28] D. Cordella, F. Ouhib, A. Aqil, T. Defize, C. Jérôme, A. Sergei, E. Drockenmüller, K. Aissou, D. Taton, C. Detrembleur, Fluorinated Poly(ionic liquid) Diblock Copolymers Obtained by Cobalt-Mediated Radical Polymerization-Induced Self-Assembly, *ACS Macro Lett* 6 (2017) 121–126, <https://doi.org/10.1021/acsmacrolett.6b00899>.
- [29] C. Fang, L. Kong, Q. Ge, W. Zhang, X. Zhou, L. Zhang, X. Wang, Antibacterial activities of N-alkyl imidazolium-based poly(ionic liquid) nanoparticles, *Polym. Chem.* 10 (2019) 209–218, <https://doi.org/10.1039/C8PY01290C>.
- [30] E. Azaceta, R. Marcilla, A. Sanchez-Diaz, E. Palomares, D. Mecerreyes, Synthesis and characterization of poly(1-vinyl-3-alkylimidazolium) ionic polymers for quasi-solid electrolytes in dye sensitized solar cells, *Electrochim. Acta* 56 (2010) 42–46, <https://doi.org/10.1016/j.electacta.2009.01.058>.
- [31] T.K. Carlisle, E.F. Wiesenauer, G.D. Nicodemus, D.L. Gin, R.D. Noble, Ideal CO₂/Light Gas Separation Performance of Poly(vinylimidazolium) Membranes and Poly(vinylimidazolium)-Ionic Liquid Composite Films, *Ind. Eng. Chem. Res.* 52 (2013) 1023–1032, <https://doi.org/10.1021/ie202305m>.
- [32] W. Yao, Y. Li, X. Huang, Fluorinated poly(meth)acrylate: synthesis and properties, *Polymer* 55 (2014) 6197–6211, <https://doi.org/10.1016/j.polymer.2014.09.036>.
- [33] K.F. Roenigk, R.K. Thery, V.J. LeMire, A.D. Otteson, G. L. Holmes, inventors; Minnesota Mining and Manufacturing Company, USA. Dye thermal transfer sheet with anti-stick coating. Publication Date 1992/08/25. US. Patent US5141915A.
- [34] E. Kissa, *Fluorinated Surfactants and Repellents*, 2nd ed., Dekker, New York, 2001.
- [35] A. Vitale, R. Bongiovanni, B. Ameduri, Fluorinated Oligomers and Polymers in Photopolymerization, *Chem. Rev.* 115 (2015) 8835–8866, <https://doi.org/10.1021/acs.chemrev.5b00120>.
- [36] J. Zhang, X. Sheng, L. Jiang, The dewetting properties of lotus leaves, *Langmuir* 25 (2009) 1371–1376, <https://doi.org/10.1021/la8024233>.
- [37] Z. Guo, W. Liu, B.-L. Su, Superhydrophobic surfaces: from natural to biomimetic to functional, *J. Colloid Interf. Sci.* 353 (2011) 335–355, <https://doi.org/10.1016/j.jcis.2010.08.047>.
- [38] J. Zhang, A. Wang, S. Seeger, Nepenthes pitcher inspired anti-wetting silicone nanofilaments coatings: preparation, unique anti-wetting and self-cleaning behaviors, *Adv. Funct. Mater.* 24 (2014) 1074–1080, <https://doi.org/10.1002/adfm.201301481>.
- [39] Z.-H. Zhang, H.-J. Wang, Y.-H. Liang, X.-J. Li, L.-Q. Ren, Z.-Q. Cui, C. Luo, One-step fabrication of robust superhydrophobic and superoleophilic surfaces with self-cleaning and oil/water separation function, *Sci. Rep.* 8 (2018) 3869, <https://doi.org/10.1038/s41598-018-22241-9>.
- [40] L.-K. Wu, J.-M. Hu, J.-Q. Zhang, One step sol-gel electrochemistry for the fabrication of superhydrophobic surfaces, *J. Mater. Chem. A* 1 (2013) 14471, <https://doi.org/10.1039/C3TA13459H>.
- [41] Y. Wang, Y. Shi, L. Pan, M. Yang, L. Peng, S. Zong, Y. Shi, G. Yu, Multifunctional superhydrophobic surfaces templated from innately microstructured hydrogel matrix, *Nano Lett* 14 (2014) 4803–4809, <https://doi.org/10.1021/nl5019782>.
- [42] A. Pozzato, S.D. Zilio, G. Fois, D. Vendramin, G. Mistura, M. Belotti, Y. Chen, M. Natali, Superhydrophobic surfaces fabricated by nanoimprint lithography, *Microelectron. Eng.* 83 (2006) 884–888, <https://doi.org/10.1016/j.mee.2006.01.012>.
- [43] C.-W. Peng, K.-C. Chang, C.-J. Weng, M.-C. Lai, C.-H. Hsu, S.-C. Hsu, Y.-Y. Hsu, W.-I. Hung, Y. Wei, J.-M. Yeh, Nano-casting technique to prepare poly(aniline surface with biomimetic superhydrophobic structures for anticorrosion application, *Electrochim. Acta* 95 (2013) 192–199, <https://doi.org/10.1016/j.electacta.2013.02.016>.
- [44] S. Pan, A.K. Kota, J.M. Mabry, A. Tuteja, Superomniphobic surfaces for effective chemical shielding, *J. Am. Chem. Soc.* 135 (2013) 578–581, <https://doi.org/10.1021/ja310517s>.

- [45] M.J. Nine, M.A. Cole, L. Johnson, D.N.H. Tran, D. Losic, robust superhydrophobic graphene-based composite coatings with self-cleaning and corrosion barrier properties, *ACS Appl. Mat. Inter.* 7 (2015) 28482–28493, <https://doi.org/10.1021/acsami.5b09611>.
- [46] C.-T. Hsieh, W.-Y. Chen, F.-L. Wu, Fabrication and superhydrophobicity of fluorinated carbon fabrics with micro/nanoscaled two-tier roughness, *Carbon* 46 (2008) 1218–1224, <https://doi.org/10.1016/j.carbon.2008.04.026>.
- [47] S. Barthwal, Y.S. Kim, S.-H. Lim, Mechanically robust superamphiphobic aluminum surface with nanopore-embedded microtexture, *Langmuir* 29 (2013) 11966–11974, <https://doi.org/10.1021/la402600h>.
- [48] J. Yong, F. Chen, Q. Yang, J. Huo, X. Hou, Superoleophobic surfaces, *Chem. Soc. Rev.* 46 (2017) 4168–4217, <https://doi.org/10.1039/C6CS00751A>.
- [49] H. Liu, J. Huang, Z. Chen, G. Chen, K.-Q. Zhang, S.S. Al-Deyab, Y. Lai, Robust translucent superhydrophobic PDMS/PMMA film by facile one-step spray for self-cleaning and efficient emulsion separation, *Chem. Eng. J.* 330 (2017) 26–35, <https://doi.org/10.1016/j.cej.2017.07.114>.
- [50] J. Li, R. Kang, X. Tang, H. She, Y. Yang, F. Zha, Superhydrophobic meshes that can repel hot water and strong corrosive liquids used for efficient gravity-driven oil/water separation, *Nanoscale* 8 (2016) 7638–7645, <https://doi.org/10.1039/C6NR01298A>.
- [51] A. Murauer, R. Bakry, G. Partl, C.W. Huck, M. Ganzera, Optimization of an innovative vinylimidazole-based monolithic stationary phase and its use for pressured capillary electrochromatography, *J. Pharm. Biomed.* 162 (2019) 117–123, <https://doi.org/10.1016/j.jpba.2018.08.054>.
- [52] R. Bakry, G.K. Bonn, D. Mair, F. Svec, Monolithic porous polymer layer for the separation of peptides and proteins using thin-layer chromatography coupled with MALDI-TOF-MS, *Anal. Chem.* 79 (2007) 486–493, <https://doi.org/10.1021/ac061527i>.
- [53] P.A. Levkin, F. Svec, J.M.J. Frechet, Porous polymer coatings: a versatile approach to superhydrophobic surfaces, *Adv. Funct. Mater.* 19 (2009) 1993–1998, <https://doi.org/10.1002/adfm.200801916>.
- [54] J. Li, Le Yang, H. Liu, G. Li, R. Li, Y. Cao, H. Zeng, Simple preparation method for hydrophilic/oleophobic coatings, *ACS Appl. Mater. Interfaces* 12 (2020) 45266–45273, <https://doi.org/10.1021/acsami.0c11596>.
- [55] B. Naier, H. Schottenberger, A. Daxenbichler, T. Bechtold, G. Partl, M. Andre, S. Kronbichler, R. Kronbichler, inventors; UNIVERSITÄT INNSBRUCK and HWK-KRONBICHLER GMBH, AT. Crosslinkable Composition and Method for Producing A Coated Article. Publication Date 2019/02/14. US. Patent US20190048203A1.
- [56] M. Hummel, B. Naier, H. Schottenberger, H. Huppertz, G. Partl, M. Noisternig, inventors; HWK-KRONBICHLER GMBH, AT. Composition comprising a fluorine-containing surfactant. Publication Date 2020/10/06. US. Patent US10792633B2.
- [57] B. Naier, H. Schottenberger, R. Bakry, G. Partl, inventors; KRONBICHLER GMBH, AT. Filter for Separating Hydrophilic and Hydrophobic Fluids and Method for the Production thereof. Publication Date 2020/05/07. US. Patent US20200139305A1.
- [58] E. Azaceta Munoz, J. Palenzuela Conde, R. Tena Zaera, E. Medina, inventors; FUNDACION CIDETEC, ES. Coatings having repellent function and use thereof. Publication Date 2019/10/24. US. Patent US20190322892A1.
- [59] G.B. Ansell, D.M. Forkey, D.W. Moore, The molecular structure of 1,3-dimethyl-2(3H)-imidazolethione (C₅H₈N₂S), *J. Chem. Soc. D* 56b (1970), <https://doi.org/10.1039/C2970000056B>.
- [60] G. Laus, V. Kahlenberg, K. Wurst, T. Müller, H. Kopacka, H. Schottenberger, Synthesis and crystal structures of new 1,3-disubstituted imidazoline-2-thiones, *Z. Naturforsch. B* 68 (2013) 1239–1252, <https://doi.org/10.5560/znb.2013-3184>.
- [61] J. Cui, W. Zhu, N. Gao, J. Li, H. Yang, Y. Jiang, P. Seidel, B.J. Ravoo, G. Li, Inverse opal spheres based on polyionic liquids as functional microspheres with tunable optical properties and molecular recognition capabilities, *Angew. Chem. Int. Edit.* 53 (2014) 3844–3848, <https://doi.org/10.1002/anie.201308959>.
- [62] E.A. Lissi, J. Aljaro, Methyl methacrylate polymerization in the presence of iodine, *J. Polym. Sci. Pol. Lett.* 14 (1976) 499–502, <https://doi.org/10.1002/pol.1976.130140811>.
- [63] P. Ghosh, A.N. Banerjee, Photopolymerization of methyl methacrylate with the use of iodine as the photoinitiator, *J. Polym. Sci. Pol. Chem.* 12 (1974) 375–386, <https://doi.org/10.1002/pol.1974.170120210>.
- [64] V.D. Sharma, M.A. Ilies, Heterocyclic cationic gemini surfactants: a comparative overview of their synthesis, self-assembling, physicochemical, and biological properties, *Med. Res. Rev.* 34 (2014) 1–44, <https://doi.org/10.1002/med.21272>.
- [65] G. Cavallo, G. Terraneo, A. Monfredini, M. Saccone, A. Priimagi, T. Pilati, G. Resnati, P. Metrangolo, D.W. Bruce, Superfluorinated Ionic Liquid Crystals Based on Supramolecular, Halogen-Bonded Anions, *Angew. Chem. Int. Edit.* 55 (2016) 6300–6304, <https://doi.org/10.1002/anie.201601278>.
- [66] A.K. Kota, G. Kwon, A. Tuteja, The design and applications of superomniphobic surfaces, *NPG Asia Mater* 6 (2014), <https://doi.org/10.1038/am.2014.34.e109-e109>.
- [67] R. Das, Z. Ahmad, J. Nauruzbayeva, H. Mishra, Biomimetic coating-free superomniphobicity, *Sci. Rep.* 10 (2020) 7934, <https://doi.org/10.1038/s41598-020-64345-1>.
- [68] T.L. Liu, C.-J.C.J. Kim, Repellent surfaces. Turning a surface superrepellent even to completely wetting liquids, *Science* 346 (2014) 1096–1100, <https://doi.org/10.1126/Science.1254787>.
- [69] M. Ao, D. Kim, Aggregation behavior of aqueous solutions of 1-dodecyl-3-methylimidazolium salts with different halide anions, *J. Chem. Eng. Data* 58 (2013) 1529–1534, <https://doi.org/10.1021/je301147k>.
- [70] R.L. Weber, Y. Ye, S.M. Banik, Y.A. Elabd, M.A. Hickner, M.K. Mahanthappa, Thermal and ion transport properties of hydrophilic and hydrophobic polymerized styrenic imidazolium ionic liquids, *J. Polym. Sci. Pol. Phys.* 49 (2011) 1287–1296, <https://doi.org/10.1002/polb.22319>.
- [71] D. Zhang, P. Xing, R. Pan, X. Lin, M. Sha, B. Jiang, Preparation and surface properties study of novel fluorine-containing methacrylate polymers for coating, *Materials* 11 (2018), <https://doi.org/10.3390/ma11112258>.
- [72] M. Boban, K. Golovin, B. Tobelmann, O. Gupte, J.M. Mabry, A. Tuteja, Smooth, all-solid, low-hysteresis, omniphobic surfaces with enhanced mechanical durability, *ACS Appl. Mat. Inter.* 10 (2018) 11406–11413, <https://doi.org/10.1021/acsami.8b00521>.
- [73] L. Cao, T.P. Price, M. Weiss, Gao Di, Super water- and oil-repellent surfaces on intrinsically hydrophilic and oleophilic porous silicon films, *Langmuir* 24 (2008) 1640–1643, <https://doi.org/10.1021/la703401f>.
- [74] B. Leng, Z. Shao, G. de With, W. Ming, Superoleophobic cotton textiles, *Langmuir* 25 (2009) 2456–2460, <https://doi.org/10.1021/la8031144>.
- [75] W. Wu, X. Wang, D. Wang, M. Chen, F. Zhou, W. Liu, Q. Xue, Alumina nanowire forests via unconventional anodization and super-repency plus low adhesion to diverse liquids, *Chem. Comm.* (2009) 1043–1045, <https://doi.org/10.1039/B818633B>.
- [76] D. Wang, X. Wang, X. Liu, F. Zhou, Engineering a Titanium Surface with Controllable Oleophobicity and Switchable Oil Adhesion, *J. Phys. Chem. C* 114 (2010) 9938–9944, <https://doi.org/10.1021/jp1023185>.
- [77] T. Sieling, J. Christoffers, I. Brand, Langmuir–Blodgett monolayers of partially fluorinated ionic liquids as two-dimensional, more sustainable functional materials and coatings, *ACS Sustain. Chem. Eng.* 7 (2019) 11593–11602, <https://doi.org/10.1021/acsschemeng.9b01496>.
- [78] R. Zhou, Y. Jin, Y. Shen, P. Zhao, Y. Zhou, Synthesis and application of non-bioaccumulable fluorinated surfactants: a review, *J. Leather Sci. Eng.* 3 (2021), <https://doi.org/10.1186/s42825-020-00048-7>.
- [79] G. Cavallo, A. Abate, M. Rosati, G. Paolo Venuti, T. Pilati, G. Terraneo, G. Resnati, P. Metrangolo, Tuning of ionic liquid crystal properties by combining halogen bonding and fluorosurfactant effect, *ChemPlusChem* 86 (2021) 469–474, <https://doi.org/10.1002/cplu.202100046>.
- [80] G. Partl, G. Laus, V. Kahlenberg, H. Huppertz, H. Schottenberger, 3,3'-(Hexane-1,6-diyl)bis(1-vinyl-4-imidazoline-2-thione), *IUCrData* 2 (2017), 170599, <https://doi.org/10.1107/S2414314617005995>.
- [81] G. Partl, G. Laus, T. Gelbrich, K. Wurst, H. Huppertz, H. Schottenberger, 3-(1*H*,1*H*,2*H*,2*H*-Perfluorooctyl)-1-vinyl-4-imidazoline-2-thione, *IUCrData* 2 (2017), 170648, <https://doi.org/10.1107/S2414314617006484>.
- [82] G.M. Sheldrick, Crystal structure refinement with SHELXL, *Acta crystallogr. C* 71 (2015) 3–8, <https://doi.org/10.1107/S2053229614024218>.
- [83] G.M. Sheldrick, SHELXT - integrated space-group and crystal-structure determination, *Acta crystallogr. A* 71 (2015) 3–8, <https://doi.org/10.1107/S2053273314026370>.